Glass Transition Phenomena in Two-Component Plastic Crystals: Study of Hexasubstituted Benzenes

Md. Shahin, S. S. N. Murthy,* and L. P. Singh

School of Physical Sciences, Jawaharlal Nehru University, New Delhi 110 067, India

Received: June 9, 2006; In Final Form: July 25, 2006

We have critically examined the relaxation that is known to occur in the crystalline phase of pentachloronitrobenzene (PCNB) and 2,3,4,5,6-pentabromotoluene using dielectric spectroscopy and differential scanning calorimetry (DSC). Within the resolution of our experimental setup, a relaxation process similar to that of the primary (or α-) relaxation is found. A slight deviation from Arrhenius behavior is noticed only in the vicinity of the glass transition temperature (T_g). This deviation and a small steplike change found in the DSC scans at T_g indicates that the "fragility" of these plastic crystals is rather low. However, in PCNB, the dielectric strength ($\Delta\epsilon$) of the above said α-process did not change appreciably with temperature, and, interestingly, a small addition of an impurity such as pentachlorobenzene (PCB) to the molten state of PCNB drastically lowered the dielectric strength and the calorimetric signature of glass transition phenomena in the DSC data at T_g. The room-temperature powder X-ray diffraction measurements in combination with the DSC data in the melting temperature region did not indicate any observable change in the crystalline structure. A residual α-process with no significant change in the shape of the dielectric spectrum indicates that the hindrance to the rotational motion of PCNB molecules is caused by the presence of a small number of PCB molecules in the crystalline lattice of PCNB over a certain region. Outside of this region, the original PCNB disordered phase is preserved, which is the origin of the residual α-process. With a further increase in PCB concentration, the α-process, characteristic of pure PCNB, vanishes, and instead another relaxation develops. This process is explained with the help of a solid−liquid phase diagram of the α-process of the plastic phase of 2:1 and 1:2 compound formations, which are stable below 386 ± 1 and 366 ± 1 K, respectively.

1. Introduction

The relaxation in supercooled plastic crystals is found[1−9] to be very similar in characteristics to that of supercooled liquids.[10−15] The main relaxation process (also called the α-process) in supercooled plastic crystals is found to be non-Debye in frequency dependence and non-Arrhenius in temperature (T) dependence[1−9] down to the glass transition temperature (T_g).[1,2,16−21] Therefore, a clear understanding of the molecular relaxation in these substances,[22−29] where only the orientational degrees of freedom are involved, is considered to be important to understand the glass transition phenomena in general. Among the plastic crystalline substances, the hexasubstituted benzenes form an interesting category as the molecular relaxation in the crystalline phase is "hindered" to varying degrees; that is, free rotation of the molecules as in the true liquid phase is not possible, and, hence, the molecules have limited rotational mobility.[30−35] These substances also are attractive to researchers of glass physics as they are composed of "rigid" non-H-bonded molecular systems and appear to be lacking the secondary (or β-) relaxation process,[35] hitherto thought[10] to be a characteristic feature of the glass transition. Brand et al.[8] have reported measurements on pentachloronitrobenzene (PCNB) over a frequency range of 14 decades, and the corresponding T dependence of the relaxation rate is found to be strictly Arrhenius. (A similar T dependence has been reported by Ries et al.[36] in proton glasses). This is an interesting observation, as the corresponding specific heat measurements[37−39] show a small steplike change at T_g, indicating that PCNB is a "less fragile glass" as per the classification of Angell.[3,11] In addition, the β-peak is either absent or submerged under the α-peak.[8,38,40] Our recent measurement[40] of the relaxation rate on the same system correlates well with that of others over most of the temperature scale but deviates from that of Brand et al.[8] near T_g. Moreover, in some of the earlier reports[30−35] on some of these systems, the T dependence of the main relaxation is stated to be Arrhenius, whereas our recent observation[40] on PCNB favors a Vogel−Fulcher−Tammann (VFT) (or power law (PL)) type of non-Arrhenius dependence. In addition, the dielectric strength, $\Delta\epsilon$, reported by different research groups is not the same, and we suspect that the presence of impurities plays an important role. Hence, the relaxation in these substances needed a critical examination both for the T dependence of the relaxation rate and the effect of impurities on the overall relaxation behavior. Presented below are the results of our study of these systems using wide frequency dielectric spectroscopy, differential scanning calorimetry (DSC) and X-ray diffraction (XRD) techniques at room temperature.

2. Experiment

The samples used in the study are PCNB and 2,3,4,5,6-pentabromotoluene (PBT) (both with a specified purity of ≥99%), and pentachlorobenzene (PCB) (purity > 98%), which were obtained from Aldrich Co. They were all used as received without any further purification.

The DSC measurements were performed using a Perkin-Elmer Sapphire DSC using a quench cooling accessory. The

* Author for correspondence. E-mail: ssnm0700@mail.jnu.ac.in.

10.1021/jp063599j CCC: $33.50
Published on Web 08/24/2006

TABLE 1: Details of the α-Process for Samples Shown in Figure 1

sample	range of temp (K)	HN parameters		PL parameters				Arrhenius equation for 100 Hz ≤ f ≤ 1 MHz	
		α_{HN}	β_{HN}	log $f_{0,\alpha}$ (Hz)	r	T_g' (K)	$T_g{}^a$ (K) (diel.)	log f_0 (Hz)	E (kJ/mol)
PBT	301−352	0.335−0.20	0.80−0.87	4.42	12.90	171.6	217.2	15.70	74.08
PCNB	276−365	0.123−0.016	0.73−0.71	4.92	12.66	166.7	206.2	15.4	67.00
PCT	186−294[b]	0.0	0.55−1.00	3.12	12.37	118.4	156.0	13.90	48.62
	210−333[c]	0.004−0.05	0.72−0.77						
1,3,4-TCTMB	182−293[c]	0.183−0.002	0.64−0.72	5.93	9.51	131.0	146.0	14.90	44.60
1,2,3-TCTMB	163−266[b]	0.15−0.61	1.00	10^{-6}	15.32	72.27	117.9	14.30	40.01
1,2-DCTMB	134−198[b]	0.33−0.15	1.00	1.76	13.06	73.2	104.6	13.7	33.5

[a] Temperature where $f_m = 10^{-3}$ Hz, calculated from PL parameters. [b] Reference 35. [c] The data were scanned from Figures 2 and 3 of Turney (ref 31) and analyzed further by us using eq 1.

DSC cell was calibrated for temperature using indium (melting transition = 429.75 K) and cyclohexane (solid−solid transition = 186.09 K) as standards. The XRD pattern of the samples was taken at room temperature using a Philips X'pert diffractometer with a CPS 120 detector. The X-ray unit was monochromatized using Cu Kα_1 (λ = 1.54056 Å) with silicon (a = 0.543088 nm) for the internal standard. For the dielectric measurements, an HP 4284A precision LCR meter in the frequency range of 20 Hz to 1 MHz was used. For frequencies in the range of 20−10^{-3} Hz, we sampled the dielectric absorption currents in the time window of 0.01−1000 s, using a digital storage oscilloscope (DSO) card DSO-2200 (Link Instruments, Inc.) in combination with a Keithley model no. 617 programmable electrometer. The complex permittivity was calculated by taking discrete Fourier transform of the discharging current. But there is a limitation in this kind of measurement, set by the resolution of the DSO card. Because of this, we are not able to determine the complete spectral characteristic at these low frequencies. However, the f_m values measured with the help of this technique are as good as those measured by the LCR bridge. For further details on the chemicals, experimental setup, and the measurements, the reader may consult our earlier articles.[40,41]

3. Results

3.1. Dielectric Relaxation in Pure Samples of Hexasubstituted Benzenes. The first-order transition temperatures and the associated enthalpies[40] are as follows: for PCNB, T_m (melting temperature) = 417.2 K, ΔH = 18.55 kJ/mol, T_1 (solid−solid transition) = 413.4 K, and ΔH = 0.57 kJ/mol; for PBT, T_m = 556.6 K and ΔH = 27.67 kJ/mol. Both PCNB and PBT are plastic crystalline solids at room temperature. In our previous report,[40] the measurements on PBT were performed on a sample in the form of a pellet of 1−2 mm thickness and about 2.5 cm in diameter. As a result, the sample capacitance and, hence, the signal-to-noise ratio was lower; therefore, we could determine the peak loss frequency f_m values over only 4 decades, that is, from 100 Hz to 1 MHz at temperatures much above T_g. As a result, deviation from Arrhenius behavior of the relaxation rate was not found, as the data of f_m values were not available in the region of T_g where such deviations are usually more pronounced. To overcome the difficulty mentioned above, we designed a concentric cylindrical capacitor whose empty cell capacitance, C_0, is about 214 pF, and the sample is melted in a vacuum to fill the capacitor plates. In the case of PBT, we could not fill the cell completely because of the difficulty associated with vaporization of the material during its melting at 556.6 K. Hence, we corrected the C_0 value for the air gaps using the ϵ' values of the sample in the form of a pellet at room temperature.

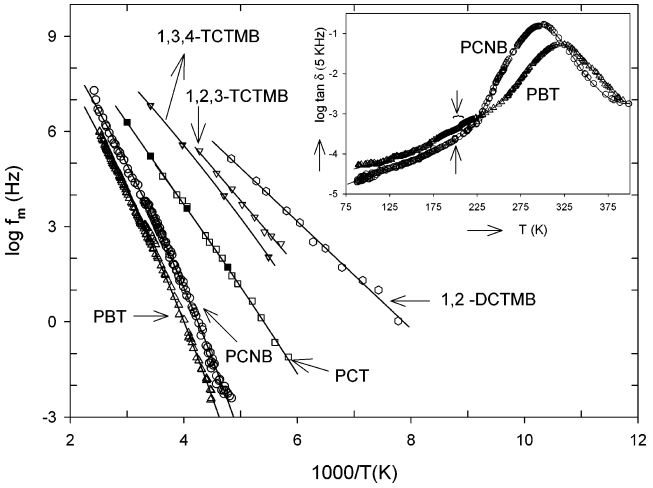

Figure 1. Arrhenius plot of f_m in the plastic phase of PCNB and PBT, where the data on other hexasubstituted benzenes [PCT (refs 31 and 35), 1,3,4-TCTMB (ref 31) and 1,2,3-TCTMB (ref 35)] is also shown for the purpose of comparison. The thick line along the experimental points corresponds to the PL, i.e., eq 2, for the parameters shown in Table 1. Also shown in the inset is the T variation of the dissipation factor (tan δ) at a test frequency of 5 kHz in the case of PCNB and PBT. The vertical arrows on the curves of the inset refer to the calorimetric T_g's measured previously in this laboratory.[40]

We tried to analyze the relaxation data using the Havriliak−Negami (HN) shape function[42] given by the equation

$$\frac{\epsilon^*(f) - \epsilon_\infty}{\epsilon_0 - \epsilon_\infty} = \left(1 + i\left(\frac{f}{f_0}\right)^{1-\alpha_{HN}}\right)^{-\beta_{HN}} \quad (1)$$

where f_0 is the mean relaxation frequency, α_{HN} and β_{HN} are the spectral shape parameters, and ϵ_0 and ϵ_∞ are the limiting dielectric constants for the process under consideration. The peak loss frequency (f_m) is then calculated from the parameters of eq 1.[43] The corresponding parameters are given in Table 1. The spectral dependence of the α-relaxation of dispersion in PCNB and PBT is similar to that reported previously[40] (hence, we have not shown the corresponding spectral dependence in this communication).

The sub-T_g or β-process, if present, is expected to be too small in these systems to be distinguishable from noise, which is more dominant at frequencies $f \leq 1$ kHz. For this reason, we have shown the temperature variation of tan δ at higher frequencies (where the noise is expected to be lower) as well in Figure 1 (inset). There is no well-resolvable β-process in our samples.

The T dependence of the relaxation rate corresponding to the primary (α-) relaxation process is examined critically over a

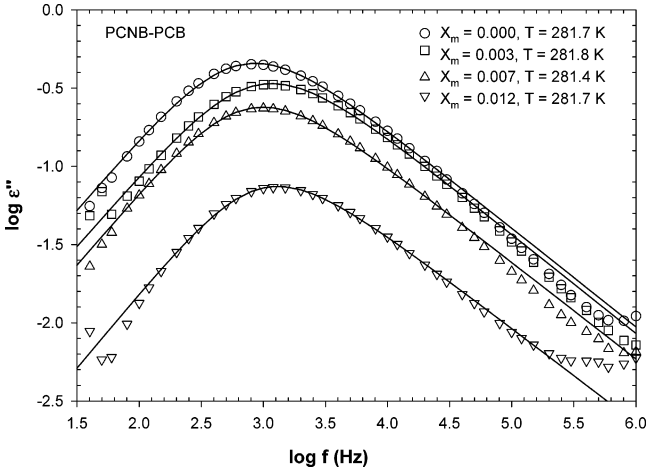

Figure 2. Double logarithmic plot of ϵ'' vs frequency of the α-process (or process I) of PCNB with an intentionally added impurity of PCB at a constant temperature. The thick line corresponds to the HN parameters discussed in the text.

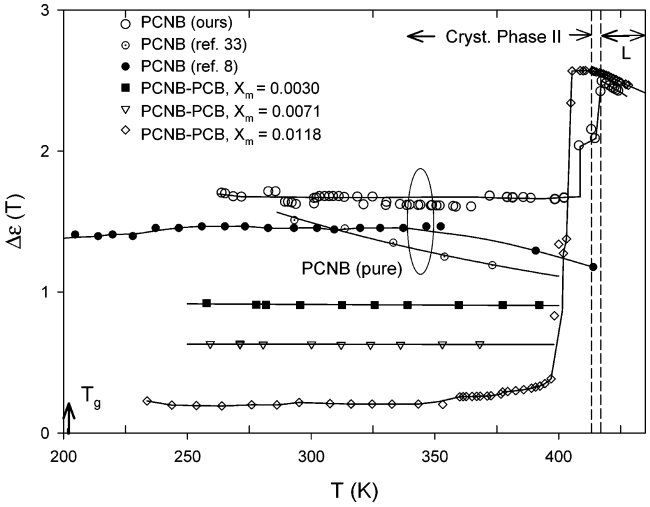

Figure 3. Effect of the intentionally added impurity (PCB) on the dielectric behavior of PCNB: T variation of the dielectric strength of the α-process. Also included are the corresponding values reported by others[8,33] for pure PCNB.

wider frequency range than that reported by us earlier.[40] The Arrhenius plot of the α-process shown in Figure 1 follows the critical PL [40] given by the equation below:

$$f_{m,\alpha} = f_{0,\alpha}\left(\frac{T - T_g'}{T_g'}\right)^r \qquad (2)$$

where $f_{0,\alpha}$ is a constant, T_g' is the limiting glass transition temperature at which $f_{m,\alpha} = 0$, and r is the dynamic exponent. It is interesting to note that the value of the exponent is around 12 (see Table 1), as is found in many supercooled liquids.[14,15,44−46] The present results are significant in view of the reported Arrhenius T dependence of the α-process in PCNB by Brand et al.[8] and in some proton glasses by Ries et al.[36] Alternately, the data can also be described equally well by the VFT equation[11] given by

$$f_{m,\alpha} = f_{0,\alpha}e^{(-B/(T-T_0))} \qquad (3)$$

where T_0 is the limiting temperature, $f_{0,\alpha}$ is a constant, and $B = E/R$, where E is the corresponding activation energy. The above equation can be reduced to the Arrhenius equation,[22]

$$f_m = f_0 e^{-(E/RT)} \qquad (4)$$

for $T = 0$. We have also tabulated the results of the fits to eqs 2 and 4 in Table 1. Also included in Figure 1 are the f_m values reported by others for some (other) hexasubstituted benzenes, which we have reanalyzed as shown in Table 1. For the temperature region for which 100 Hz $\leq f_m \leq$ 1 MHz, within the accuracy of our data, it is difficult to say whether an Arrhenius fit (eq 4) is a better fit to the data than both the VFT and PL fits. However, a careful study of eq 4 in Table 1 reveals that the corresponding f_0 is much larger than $10^{12}-10^{13}$ Hz (lattice vibrational frequency). Hence, from Figure 1, one can infer that, with increase in the size of the hexasubstituted benzene, the behavior gradually crosses over from nearly Arrhenius to a non-Arrhenius temperature dependence.

3.2. Effect of Impurities on the α-Process of PCNB. Interestingly, the addition of impurities such as PCB drastically lowered the $\Delta\epsilon$ values for the pure PCNB, as can be observed in Figures 2 and 3. Our dielectric measurements on PCB revealed that the material is a rigid crystalline solid at room temperature. This, together with our DSC measurements, shows

TABLE 2: Details of Eq 1 in Figure 2.

x_m[a]	temp	α_{HN}	β_{HN}	f_0 (Hz)	f_m (Hz)	$\Delta\epsilon$
0.00	281.7	0.0745	0.6844	6.12×10^2	0.856×10^3	1.2156
0.003	281.8	0.0845	0.6926	8.38×10^2	1.166×10^3	0.9105
0.007	281.4	0.0664	0.6625	6.92×10^2	0.992×10^3	0.6402
0.012	281.7	0.0440	0.6322	8.85×10^2	1.302×10^3	0.1977

[a] Mole fraction of PCB.

that it crystallizes to a non-rotator-phase solid in one step, with a corresponding melting transition temperature of 357.7 K. This material was chosen because of its higher melting temperature, thus it can readily be mixed with molten PCNB without evaporation. Shown in Figure 2 is the relaxation spectrum of disordered PCNB phase at a particular temperature for various concentrations of PCB. The spectrum is well represented by eq 1 with little variation in the spectral shape parameters (see Table 2). Depicted in Figure 3 is the temperature variation of the dielectric strength of both pure and impure samples of PCNB with small amounts of PCB. Also included in the same figure are different data reported by various groups, including that of the PCNB sample of Aihara et al.,[33] which was purified by repeated recrystallization. Our dielectric measurements show a drastic decrease in the $\Delta\epsilon$ values without any observable change in the f_m values and the shape of the dielectric spectrum, as shown in Figure 2. However, with PCB as the impurity, we observed another process (designated as process II) on the higher frequency or lower temperature side, as shown in Figure 4. To understand the nature of this process and its relationship to the phase behavior of the sample, we critically monitored the thermal behavior using DSC and the corresponding dielectric behavior of the sample during very slow heating. The corresponding results are shown in Figures 5 and 6. The DSC scans in the region of melting (Figure 5) do not show any drastic change in the phase behavior. We also critically examined the T_g region in the DSC scans of these samples (inset of Figure 5), which reveals that the signature of the glass transition at T_g, that is, the change of baseline at T_g, is reduced for PCNB with a 0.01 mole fraction of PCB. Plotted in Figure 6 is the real part of the dielectric constant at various frequencies along with the static dielectric constant determined from eq 1. Data plotted in this way gives us immediate information about the thermodynamic transitions. From Figure 6 we see a lowered dispersion for the impure sample, and the dielectric strength $\Delta\epsilon$ of the

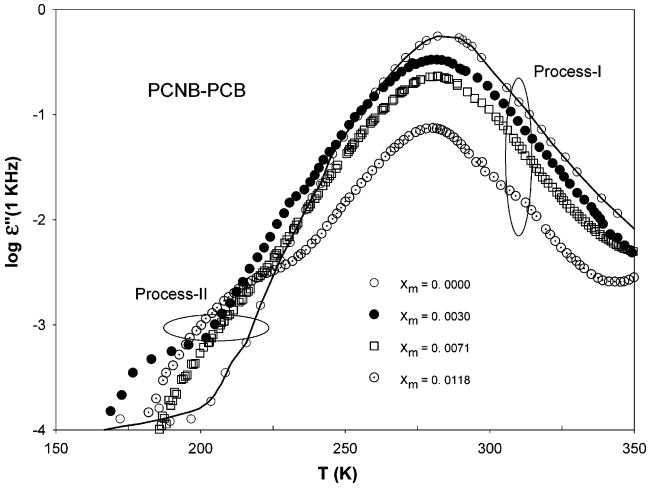

Figure 4. Variation of ϵ'' with temperature at a test frequency of 1 kHz, in samples of PCNB for smaller concentrations (x_m) of PCB. The thick lines are a guide to the eye. Note that process I is increasingly diminished with PCB impurity, and a low-temperature process designated as process II appears in samples for $x_m > 0.0071$.

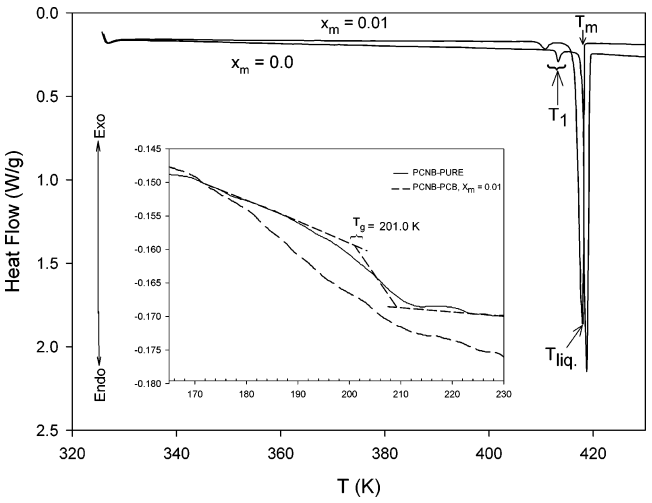

Figure 5. DSC curves of PCNB with PCB as the impurity: the DSC scans above room temperature up to the melting temperature for a heating rate of 2°/min. The sample sizes are 11.4 and 10.2 mg, respectively. Shown in the inset is a portion of the DSC curves taken for a heating rate of 10°/min in the region of the glass transition temperature. (The curves are aligned along the *Y*-axis as per the software supplied along with the DSC instrument to make the comparison easier.)

sample with an impurity of PCB goes back to the original value of PCNB on "rotational and positional melting" at T_1 and T_m respectively. The inference from the DSC behavior shown in Figure 5 is further supported by the corresponding X-ray diffractograms at room temperature (Figure 7), which did not indicate noticeable change in the lattice structure for smaller concentrations of PCB.

3.3. Dielectric Behavior of PCNB in the Presence of Larger Concentrations of PCB. To better understand the origin of process II found in PCNB in the presence of smaller concentrations of PCB, we studied the X-ray, thermal, and dielectric behavior of the PCNB−PCB binary system at higher concentrations. The X-ray results are included in Figure 7 for easy comparison. For the determination of dielectric behavior, the samples were slowly cooled in the dielectric cell from the liquid phase to room temperature at an approximate rate of 1°/min, and then annealed at room temperature for 4−6 h.

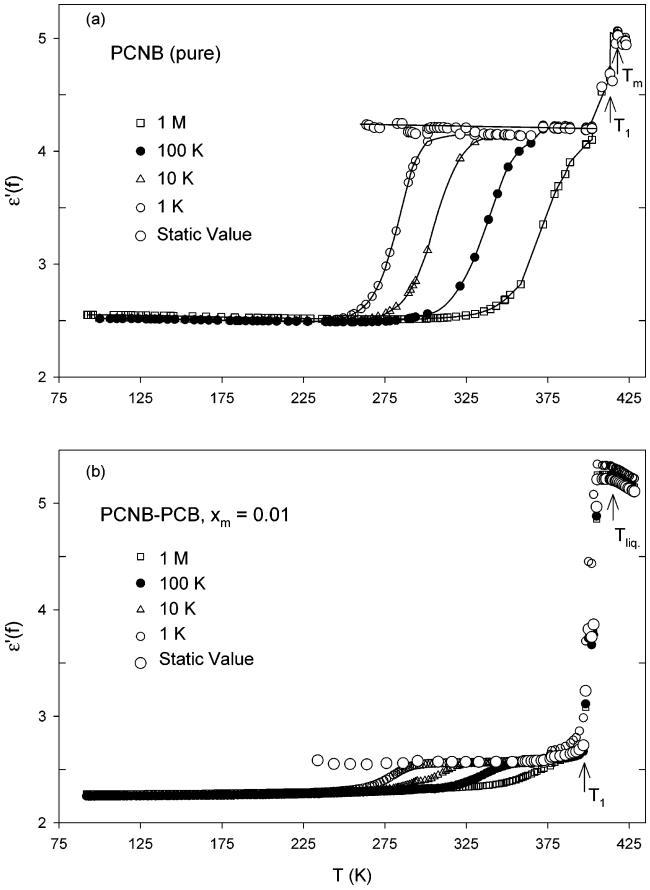

Figure 6. Effect of PCB as the impurity upon the dielectric behavior of PCNB: the variation of ϵ' with T for different frequencies where T_{liq} is the liquidus temperature as defined in eq 5.

Dielectric measurements were taken isothermally after the samples were cooled to liquid nitrogen temperature. Depicted in Figure 8 is the T variation of ϵ'' at a fixed frequency for various x_m (mole fraction of PCB) values, where an increase in the magnitude of process II with increasing x_m and an almost complete disappearance of process I for $x_m \geq 0.33$ are evident. To make obvious the spectral shape of the relaxation, we have shown the spectral behavior of two samples of different x_m values in Figure 9, where the α-process can reasonably be explained by eq 1 around the peak frequency region, and the corresponding parameters of the approximate fits are given in Table 3. However, within the resolution of our experimental setup, we have not found any resolvable β-process in these samples. Although we are able to force fit the data to the HN function for the peak frequency, region deviations from eq 1 are noticeable at the asymptotic regions. Therefore, it would be much more meaningful to look at the spectral half-widths, and, hence, the temperature variation of this parameter for some samples is shown in Figure 10. The complete relaxation map of the samples is shown in Figure 11, depicting f_m values in the form of an Arrhenius diagram. The T variation of the $\Delta\epsilon$ values corresponding to processes I and II is shown in Figure 12 for all the samples studied covering the entire concentration range of $0 \leq x_m \leq 1$. The rapid crystallization of samples from their liquid phase may have given rise to an error of about 10% in the actual values of $\Delta\epsilon$, (probably because of improper filling of the cell). It is with this limitation that the values of $\Delta\epsilon$ were looked at.

To support the interpretation of our dielectric results, we have also performed DSC measurements over the complete concentra-

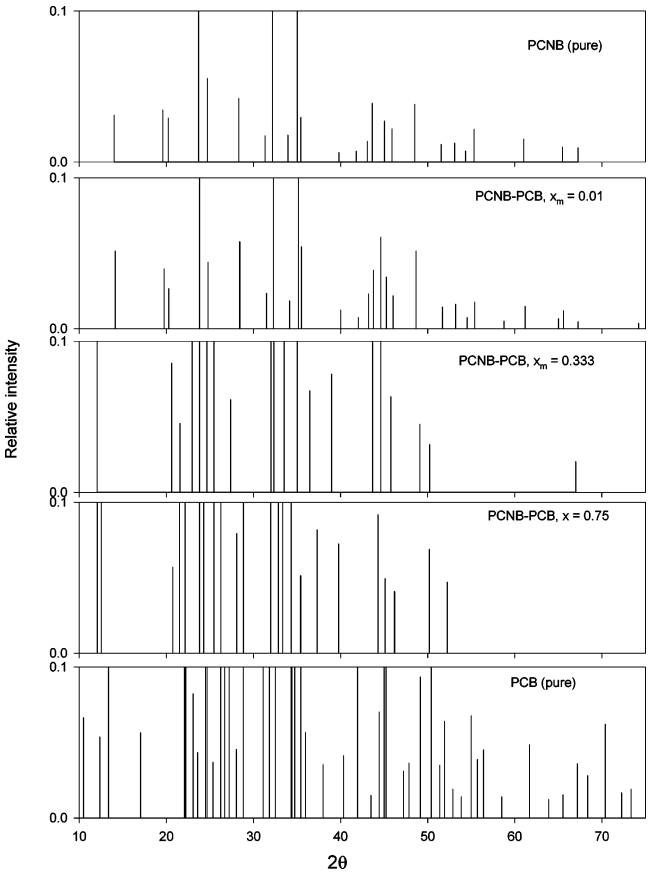

Figure 7. Powder X-ray diffractograms at room temperature for the samples with $x_m = 0.01$, 0.333, and 0.75 along with diffractograms corresponding to pure PCNB and PCB.

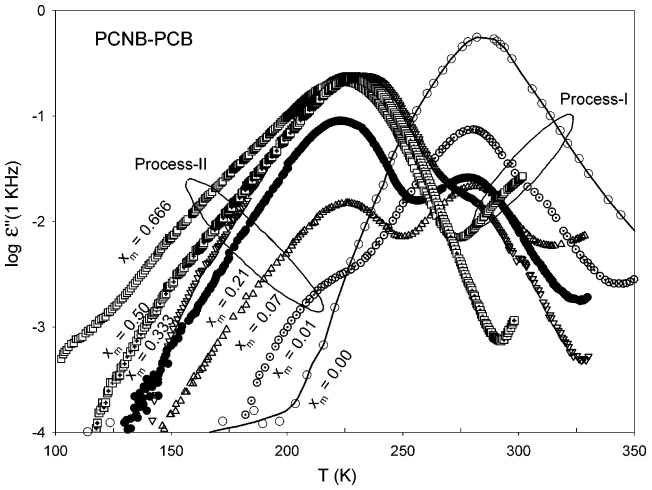

Figure 8. PCNB−PCB binary system: Variation of ϵ'' with temperature at a test frequency of 1 kHz, for various concentrations of PCB. The thick lines are a guide to the eye. Note that process I is very small or almost absent for $x_m > 0.333$, and process II dominates the relaxation in samples for $x_m > 0.10$.

tion range in the PCNB−PCB binary system. Some of the DSC curves are shown in Figure 13, and the corresponding phase diagram is shown in Figure 14. The DSC scans taken during heating at a rate of 2°/min were analyzed by determining the onset temperature (T_2) and end temperature (T_l) of the endotherms shown in Figure 13 using the DSC Instrument software. The transition temperatures thus determined are plotted as a function of the mole fraction of PCB (x_m), as suggested in refs 47−49, to determine the solid−liquid phase diagram. The DSC scans of

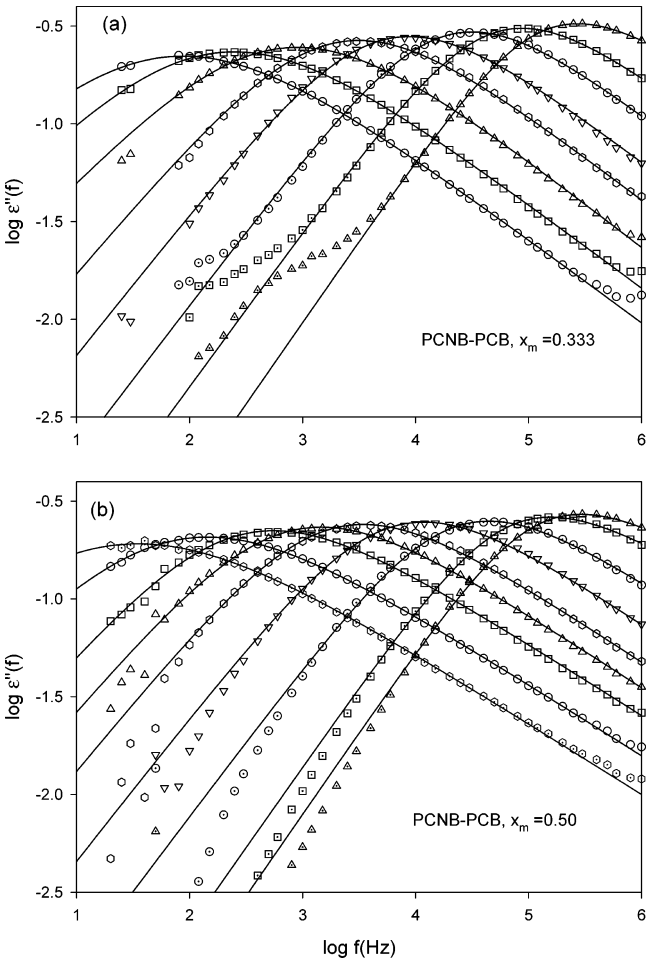

Figure 9. Double logarithmic plot of ϵ'' vs frequency of process II in the PCNB−PCB binary system at PCB concentrations of (a) $x_m = 0.333$ (210.5 K $\leq T \leq$ 275.5 K) and (b) $x_m = 0.50$ (208.3 K $\leq T \leq$ 272.8 K). The thick line corresponds to the HN parameters shown in Table 3. Deviation from the HN equation in the lower frequency side in panel a may be due to the presence of residual process I.

TABLE 3: Details of Eq 1 for Samples Shown in Figure 9

x_m	temp	α_{HN}	β_{HN}	f_0 (Hz)	f_m (Hz)	$\Delta\epsilon$
0.333	194.1				2.80×10^0	
	199.8				9.50×10^0	
	210.5	0.433	0.755	5.49×10^1	8.72×10^1	1.031
	217.3	0.403	0.725	1.50×10^2	2.47×10^2	1.041
	225.1	0.388	0.738	5.68×10^2	8.99×10^2	1.058
	238.8	0.312	0.642	1.77×10^1	3.17×10^3	1.065
	246.4	0.271	0.604	4.75×10^3	8.79×10^3	1.070
	257.1	0.239	0.587	1.71×10^4	3.17×104	1.088
	265.2	0.207	0.548	4.54×10^4	8.79×104	1.118
	275.8	0.146	0.436	1.18×10^5	2.70×10^5	1.213
0.500	190.1				8.25×10^{-1}	
	200.1				6.33×10^0	
	208.3	0.465	0.679	1.77×10^1	3.50×10^1	0.990
	215.9	0.392	0.602	6.66×10^1	1.44×10^2	0.980
	223.9	0.329	0.547	2.45×10^2	5.54×10^2	0.986
	230.0	0.315	0.551	6.63×10^2	1.46×10^3	1.001
	236.4	0.291	0.541	1.59×10^3	3.46×10^3	1.002
	245.7	0.262	0.527	5.49×10^3	1.19×10^4	0.995
	256.9	0.230	0.494	1.99×10^4	4.46×10^4	0.989
	267.6	0.174	0.405	6.07×10^4	1.56×10^5	1.061
	272.8	0.161	0.389	1.11×10^5	2.92×10^5	1.100

the sample shown in Figure 13 clearly reveal that, above the transition temperature T_2 (= 387.3 ± 1 K) in the concentration range $0.01 \leq x_m \leq 0.333$, the S_{II} phase (which is a 2:1 compound of PCNB and PCB) is in equilibrium with the liquid. This is also confirmed by the fact that the liquidus line follows

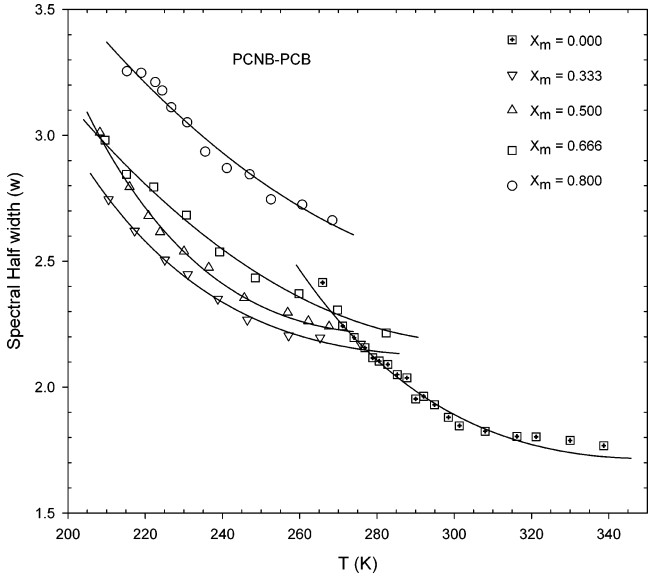

Figure 10. PCNB−PCB binary system: temperature variation of the half-width of the dielectric loss spectra.

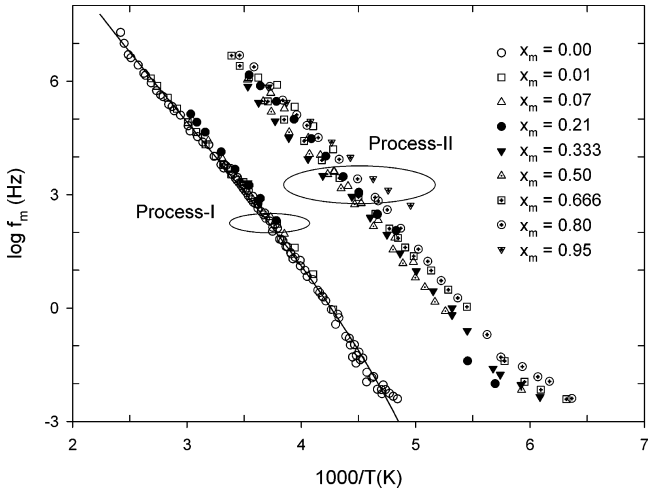

Figure 11. PCNB−PCB binary system: Arrhenius plot of the f_m values corresponding to processes I and II.

the equation for the depression of freezing point for ideal solutions[50] given by

$$\ln(x_m) = \frac{\Delta H_f}{R}\left(\frac{1}{T_{liq}} - \frac{1}{T_m}\right) \quad (5)$$

where T_m is the melting temperature, ΔH_f is the enthalpy of melting of PCNB, and T_{liq} (or $T_{liquidus}$) is the freezing (liquidus) temperature if allowance is made for a 2:1 compound formation in the above equation. We have evidence for a 2:1 and probably a 1:2 compound formation in the phase diagram, where these compounds are unstable above the temperatures respectively depicted as T_2 and T_4 in Figure 14. For a more meaningful discussion, the details of the proposed nature of various phase transitions are given in Table 4. Interestingly, as in pure PCNB, the 2:1 compound undergoes a hindered transition at temperature T_3 with a small enthalpy change, as shown in Figure 15, which can be seen in both the DSC and dielectric behavior of the sample with a mole fraction (x_m) of 0.333 of PCB. It is evident from Figure 15 that process II is characteristic of this hindered phase, which, for most concentration ranges, is a mixed crystal system, as shown in Figure 14 (and Table 4). We have also

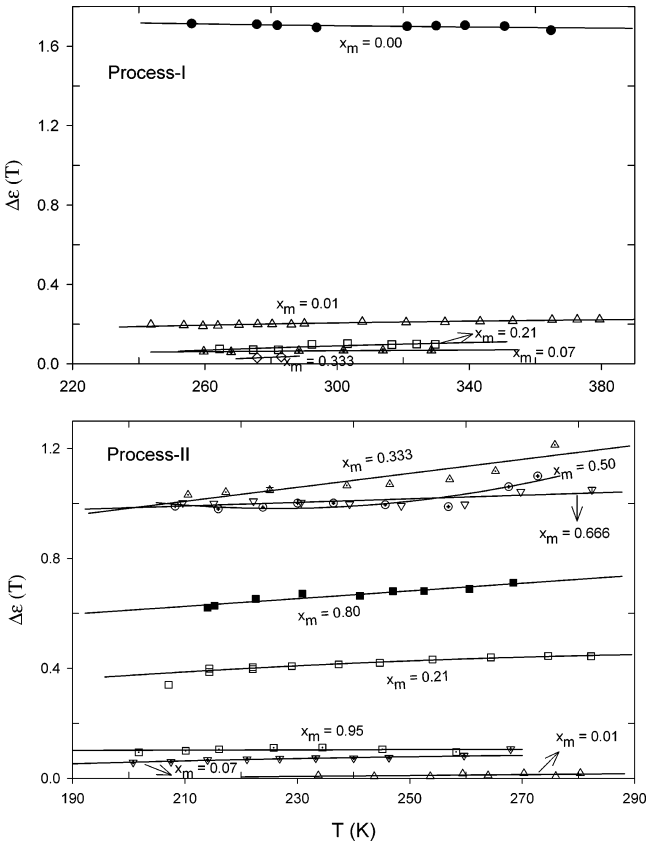

Figure 12. PCNB−PCB binary system: temperature variation of dielectric strength ($\Delta\epsilon$) corresponding to processes I and II.

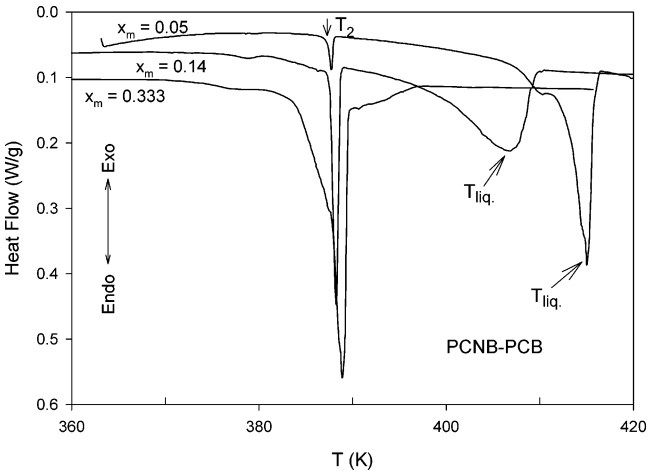

Figure 13. PCNB−PCB binary system: DSC curves for a heating rate of 2°/min for three concentrations ($0.015 < x_m \leq 0.333$). The sample sizes are for $x_m = 0.05$ (11.90 mg), $x_m = 0.14$ (10.10 mg), and $x_m = 0.33$ (12.50 mg). Note that the endotherm at T_2 increases in intensity with x_m.

confirmed this by examining the room-temperature X-ray diffractograms of the samples of different concentrations of PCB in PCNB.

4. Discussion

For the sake of convenience, the results are discussed under the following sections.

4.1. Glass Transition and α-Process in Hexasubstituted Benzenes. The relaxation observed in the two materials, viz., PCNB and PBT, is not strictly Arrhenius in nature (Figure 1), down to T_g. Moreover, a comparison of Figures 1 and 6 reveals

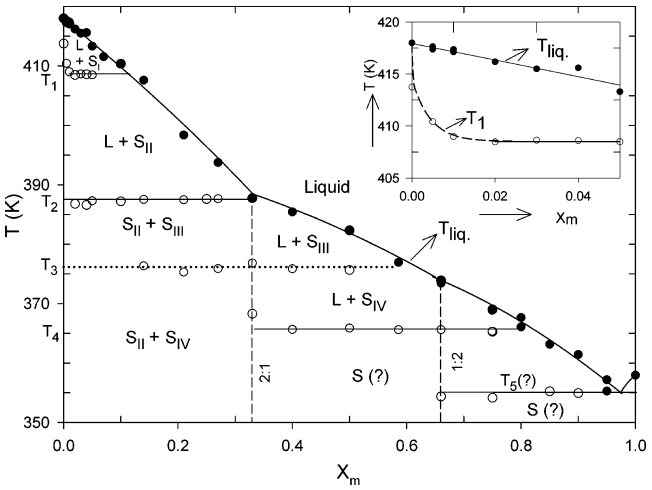

Figure 14. PCNB−PCB binary system: solid−liquid phase diagram. The upper thick line corresponds to the liquidus points (or T_{liq}). Note that, for $0.015 < x_m \leq 0.333$, the phase diagram is eutectic with incongruent melting at T_2, and the corresponding liquidus line follows eq 5. The actual nature of phase diagram is not clear in the regions shown with a ? mark (also see Table 4). In the diagram, S_I, S_{II}, etc. stand for individual crystalline solids, whereas S can be a mixture of crystalline solids. Also shown in the inset is the magnified portion of the phase diagram for $0.0 < x_m \leq 0.05$.

that, in the case of PCNB (and PBT), the kinetic freezing temperature of the α-process corresponds to T_g determined in the DSC experiments (which corresponds to an approximate log f_m value of -2.55 ± 0.45 for the enthalpy relaxation[51]). These observations clearly suggest that the relaxation process seen in the plastic phases of PCNB and PBT corresponds to the α-process, whose kinetic freezing causes the glass transition event, as also happens in glassy crystals such as cyclooctanol, cyanoadamantane, and so forth.[1] It is very clear from the inset of Figure 1 that the β-process is too small to be observed, and it is doubtful that it exists as a separate process from the α-process (the reader may refer to ref 38 for more details on this issue). Similar is the case with the binary system of PCNB−PCB (see Figures 8 and 9).

From Figure 1 and Table 1, we see that the PL equation describes the data satisfactorily. Interestingly to the data 100 Hz $\leq f_m \leq$ 1 MHz, even the Arrhenius equation describes the data within the experimental accuracy. Moreover, the apparent activation energy as defined by the Arrhenius equation reflects the changes in the molecular geometry as in the case of liquids;[22,41] it increases with increase in the size of the molecule, and decreases with increase in the number of methyl groups on the benzene ring. A similar trend can also be seen in the $T_g(D)$ values, where $T_g(D)$ is the temperature at which the f_m value is 10^{-3} Hz. Although we see a near constancy in the values of r in the PL parameter similar to that observed in the case of supercooled liquids,[14,15,44−46] presently, it is difficult to attribute any significance to this observation. The results shown in Figure 1 and Table 1 perhaps give us a clue that there is a change from Arrhenius to non-Arrhenius behavior as the size of the molecules is increased, which would then be clearly noticeable near T_g. Interestingly, in the case of the last two samples, viz., 1,2-dichlorotetramethyl benzene (1,2-DCTMB) and 1,2,3-trichlorotrimethyl benzene (1,2,3-TCTMB) given in Table 1, which are Arrhenius in the T dependence of the relaxation rate, the corresponding dielectric spectra show a symmetrical Cole−Cole type of spectral shape[22] as compared to the other samples, which are asymmetric in their spectral shape. Also, the latter group of materials has an f_0 value significantly different from the lattice vibrational frequency, indicating some "cooperativity" among the constituent molecules. The DSC scans of these samples taken by us along with the data reported by Brot and Dermon[35] do not show any collapse to a higher ordered state. One reasonable explanation that can be offered for the lack of an ordered state in PCNB and PBT is that the corresponding transitions are probably located below their respective glass transition temperatures where the rotational relaxation times are too large to effect a transition to a higher ordered state.

4.2. Effect of Impurities on the α-Process of PCNB. From the discussion given in the previous section, it is clear that disorder freezes at low T with some residual entropy. Can this be removed to some extent by doping the crystal with some impurity, as in the case of ices and ice clathrates?[53−55] Moreover, the dielectric strength $\Delta\epsilon$ of PCNB reported by different groups did not exactly tally as shown in Figure 3. (Similar is the case with the sample PCT reported by two different research groups, namely, Turney[31] and Brot and Dermon.[35]) Interestingly, the magnitude of $\Delta\epsilon$ decreased drastically with an initial increase in the concentration of the solute, as shown in Figure 3, and the corresponding spectral shape or relaxation rate did not deviate much from that of the pure PCNB (designated as process I), as shown in Figure 2. According to the X-ray measurements [56,57] at room temperature, pure PCNB crystals are rhombohedral, space group $R\bar{3}$, with cell dimensions $a_{hex} = 8.7512$ Å, $c_{hex} = 11.1115$ Å (from ref 56) and $a_{hex} = 8.769$ Å, $c_{hex} = 11.209$ Å (from ref 57). The molecular orientation is disordered in the sense that the six substituent positions round the benzene ring are indistinguishable, but free rotation of the molecules is excluded.[57] Our dielectric measurements confirm hindered rotation below a temperature T_1 of 413.4 K (see Figure 6), and, according to the X-ray measurements by Rössell and Scott,[57] the structure above this temperature is probably triclinic with freely rotating molecules. However, Rössell and Scott[57] report the transition temperature to be 408 K, which is 5.4 degrees below that of ours, and an enthalpy change of 628 J/mol as compared to our measurement[40] of 570 J/mol. Our dielectric measurements shown in Figure 6 along with the DSC results of the same samples shown in Figure 5 clearly indicate that, for temperatures $T_1 < T < T_{liq}$, the sample consists of more or less freely rotating molecules that get hindered below T_1, and the hindrance is mainly due to the presence of an impurity atom on the PCNB lattice site. Our analysis of the pure PCNB data using Crysfire 2002 software[58] gives a rhombohedral structure with $a_{hex} = 8.7745$ Å, $c_{hex} = 11.2571$ Å, with a unit cell volume of 750.6 Å^3. Thus, our X-ray analysis of the pure PCNB agrees well with that of Rössell & Scott[57] and Tanaka et al.[56] With this confidence, we have analyzed the data of the doped sample, which gives $a_{hex} = 8.7564$ Å, $c_{hex} = 11.1926$ Å, with a unit cell volume of 743.2 Å^3, indicating a slight contraction of the unit cell. A closer examination of our DSC curves (see Figure 5 and also Figure 14) in the region of melting revealed that there is a slight decrease in the transition temperature T_1 from 413.4 to 408.4 K with an increase in PCB, which may partially be accounted for by the contraction of the unit cell as described above. However, we admit that we were unable to measure the corresponding enthalpy of transition at T_1 (in doped PCNB) with a definite accuracy, as it is too small to be accounted for, and the corresponding endotherm lost its sharpness. However, interestingly, the change in the baseline of DSC at T_g in PCNB samples with PCB impurity falls very much below that of the pure PCNB samples (inset of Figure 5). The presence of a residual α-process with out any noticeable change in the shape of the dielectric spectra indicates that this residual process has

TABLE 4: Details of the Solid−Liquid Phase Diagram in the PCNB−PCB Binary System[a]

concentration range (x_m)	transition temp (K)	nature of transition[b]	other remarks
$x_m = 0$, pure PCNB	417.2	melting transition L → S_I	S_I is perhaps triclinic.[c]
	413.4 (T_1)	$S_I \rightarrow S_{II}$	S_{II} is highly hindered[d]
$0 < x_m \leq 0.015$	$413.4 < T_1 < 408.4$	$S_I \rightarrow S_{II}$	S_{II} (rhombohedral) as in pure PCNB. It is a solid solution of PCB in PCNB.[d]
$0.015 < x_m \leq 0.33$	387.3 ± 1 (T_2)	dissociation temperature of S_{III} (2:1 compound)	S_{III} is a rotational solid. Free rotation is possible for $T_2 < T < T_3$.[e]
$0.015 < x_m < 0.60$	376.0 ± 1 (T_3)	$S_{III} \rightarrow S_{IV}$	S_{IV} is rotationally hindered S_{III}.
$0.33 < x_m < 0.80$	366.0 ± 1 (T_4)	dissociation temperature of S_V (1:2 compound ?)	S_V is a rotational solid.
$0.66 < x_m < 1.0$	354.8 ± 1 (T_5)	eutectic temperature of S_V and solid PCB ?	

[a] x_m is the mole fraction of PCB. [b] L stands for liquid, and S stands for crystalline solid. [c] See ref 57. [d] See Figures 3 and 6. [e] See Figure 15.

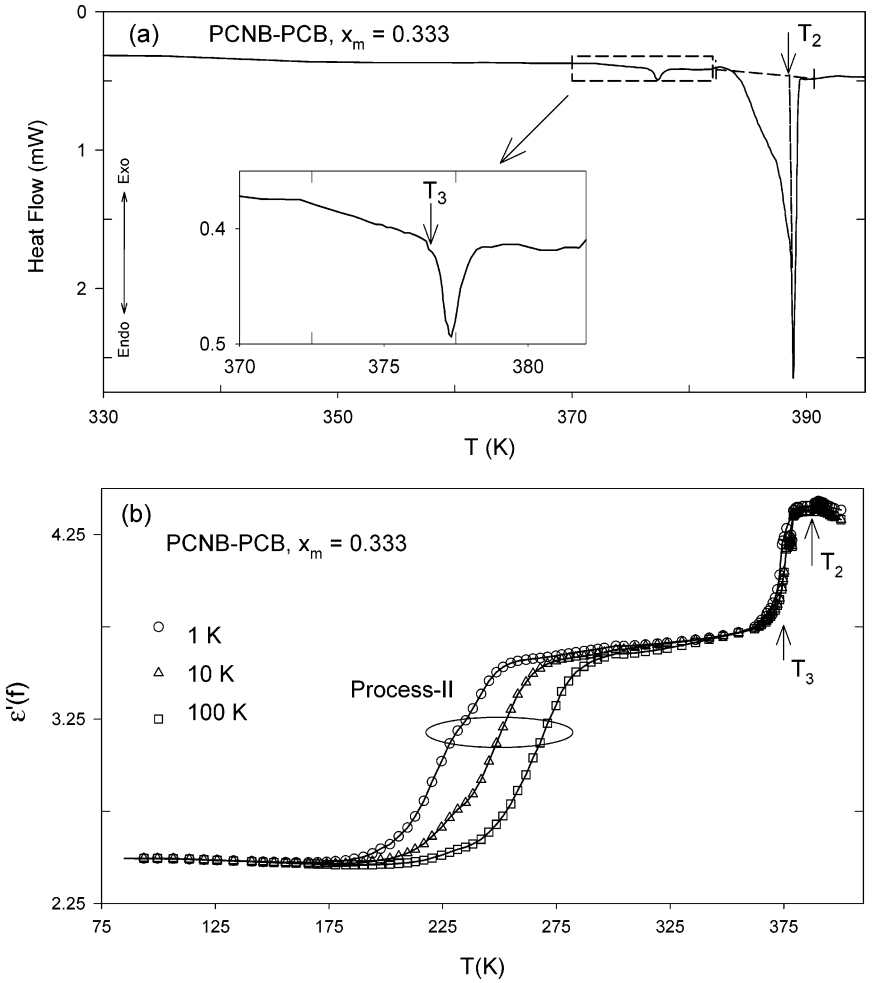

Figure 15. PCNB−PCB binary system with $x_m = 0.333$. (a) The DSC curve for a heating rate of 2°/min; Sample size, 3.40 mg. The inset in panel a is the magnified portion of the DSC curve to highlight the transition at T_3 (also see Table 4). (b) The corresponding dielectric behavior. Note that the transition at T_2 is a minor event in the dielectric behavior.

resulted from regions outside the hindered regions; the rotation of PCNB molecules inside is completely blocked by the presence of the PCB impurity on the lattice sites of PCNB.

4.3. Relaxation in the Plastic Phase(s) of the PCNB−PCB System. The complete phase diagram given in Figure 14 reveals that there is a 2:1 compound formation for $0.01 \leq x_m \leq 0.6$, which is unstable above 387.3 K. This compound is a plastic crystal below this temperature, and it seems to undergo a transition at 376.0 ± 1 K (= T_3), below which it is in a hindered orientational disordered state, as can be inferred from a comparison of the dielectric data with the calorimetric data shown in Figure 15. The corresponding X-ray diffractograms at room temperature taken by us also confirm that the structure of this solid phase at room temperature is very much different from that of the PCNB and PCB phases.[59−61] (The preliminary analysis of the corresponding X-ray diffractogram with $x_m = 0.333$ shown in Figure 7 using Crysfire software indicates that the crystal structure is monoclinic or triclinic, which is usually found in hexasubstituted benzenes.[59−61] However, this needs to be confirmed, as there can be an error in analyzing the XRD data of powder samples.) From Figures 14 and 15, we infer that the dielectric relaxation process designated as process II,

seen in the PCNB−PCB system for $x_m \geq 0.05$, may actually be due to the above hindered phase S_{IV} of the 2:1 compound for $x_m \leq 0.33$ and a mixed phase of 2:1 and 1:2 compounds for $0.33 \leq x_m \leq 0.666$ (see Figure 14). The shape of the corresponding relaxation spectra, as shown in Figures 9 and 10 and Tables 3 and 4, is very broad with a large value for α_{HN} and spectral half-width. Another note worthy feature of the relaxation in these systems is that the secondary process is too low in magnitude (Figures 8 and 9), as the dielectric spectra can reasonably be ascribed to one process, that is, process II over the entire frequency range (Figure 9, Table 3).

4.4. *T* Dependence of f_m and $\Delta\epsilon$ in the PCNB−PCB Binary System. One significant feature of all these samples is that the $\Delta\epsilon$ values corresponding to both processes I and II do not change much with temperature (Figure 11c), whereas, in an unhindered rotation, a variation in this quantity as $1/T$ is expected, as in the case of a liquid. Interestingly, all these samples undergo a small transition a few degrees below their melting (or freezing) temperature as, for example, PCNB at T_1 and the 2:1 compound at T_3 (Figure 5). The corresponding enthalpy (although it could not be determined exactly) is very low and is always around ∼300−600 J/mol. The phase diagram for binary PCNB−PCB is not clear for concentrations above $x_m = 0.666$ (see Table 4). However, we are in a position to comment that the transition at T_4 is perhaps the dissociation temperature of a 1:2 compound as the corresponding endotherm increases in magnitude with x_m in the region $0.333 \leq x_m \leq 0.666$. The 1:2 compound is also an orientationally disordered state whose relaxation overlaps that of the 2:1 compound, as is evident from Figures 8−12 and 15.

The *T* dependence of f_m is non-Arrhenius, as can be seen from the fact that, apart from a better fit to the PL (or VFT) equation, the preexponential factors for the Arrhenius equation are much larger than $10^{12}-10^{13}$ Hz, and cannot reasonably be accounted for by the lattice vibrational frequency. In fact, the f_m values of process II shown in Figure 11, if explored by eq 4 (independently for each x_m), yield very high values of f_0 in the range of $10^{16}-10^{19}$ Hz, very much in excess of the lattice vibrational frequency, indicating some cooperativity, with the corresponding *E* values ranging from 60 to 69 kJ/mol, which are of the same magnitude as that of PCNB. However, DSC scans of these samples do not clearly indicate a clear steplike change at the corresponding glass transition region, indicating that these samples are "less fragile", as is the case with mixtures of cyanoadamantane and chloroadamantane.[62,63]

5. Conclusions

(i) The hexasubstituted benzenes or their binaries do not reveal any well resolved secondary relaxation in their plastic crystalline phases within the resolution of our experimental setup.

(ii) The *T* dependence of the relaxation rate deviates from Arrhenius character near T_g in PBT, PCNB, and PCT.

(iii) Of the above hexasubstituted benzenes, only PCNB was studied near T_g using either DSC or calorimetry. The glass transition event at T_g in terms of change in specific heat, that is, $\Delta Cp(T_g)$, is about 12−15 kJ/mol/K.[37,39] This value for $\Delta Cp(T_g)$ (in units of J/mol/K) is much smaller than that of the orientationally disordered phases of *cis*-1,2-dimethylcyclohexane(∼63),[52] 2,3-dimethylbutane(51),[52] and isocyanocyclohexane,[64] but is also smaller than that of cyanoadamantane(25).[65] Thus, the system may be categorized as a less fragile system, as is the case with cyanoadamantane.[65] This is also the case with PBT,[40] where the glass transition event is hardly recognizable in the DSC data. These observations together with a smaller deviation from Arrhenius behavior place the hexasubstituted benzenes among the less fragile systems.

(iv) There is a small endothermic transition with an enthalpy on the order of about 300−600 J/mol, below which the rotation of the molecules in PCNB and its binary with PCB, that is, the PCNB−PCB system, is very much hindered, but, interestingly, the corresponding $\Delta\epsilon$ values do not change appreciably with temperature.

(v) Our observation of an increase in the hindrance of PCNB molecules in their own matrix upon doping with PCB indicates that the presence of PCB molecules on the lattice can alter the relaxation strength drastically. This result may be of interest to researchers working with binary mixtures of materials that form glassy crystals.[9,65]

Acknowledgment. L.P.S. wishes to thank CSIR, India, for Senior Research Fellowship (SRF).

References and Notes

(1) Tyagi, M.; Murthy, S. S. N. *J. Chem. Phys.* **2001**, *114*, 3640.
(2) Murthy, S. S. N. *Thermochim. Acta* **2000**, *359*, 143.
(3) Angell, C. A. *J. Non-Cryst. Solids* **1991**, *13*, 131.
(4) Leslie-Pelecky, D. L.; Birge, N. O. *Phys. Rev. Lett.* **1994**, *72*, 1232.
(5) Benkhof, S.; Kudlik, A.; Blockwicz, T.; Rössler, E. *J. Phys.: Condens. Matter* **1998**, *10*, 8155.
(6) Fuchs, A. H.; Virlet, J.; Andre, D.; Szwarc, H. *J. Chim. Phys. Phys.-Chim. Biol.* **1985**, 82, 293.
(7) Leslie-Peleckey, D. L.; Birge, N. O. *Phys. Rev. B* **1994**, *50*, 13250.
(8) Brand, R.; Lunkenheimer, P.; Loidl, A. *J. Chem. Phys.* **2002**, *116*, 10386.
(9) Tamarit, J. L.; Lopez, D. O.; de la Fuente, M. R.; Perez-Jubindo, M. A.; Salud, J.; Barrio, M. *J. Phys.: Condens. Matter* **2000**, *12*, 8209.
(10) Johari, G. P. *Ann. N.Y. Acad. Sci.* **1976**, *279*, 117.
(11) Wong, J.; Angell, C. A. *Glass Structure: By Spectroscopy*; Marcel Dekker: New York, 1976.
(12) Williams, G. In *Dielectric and Related Molecular Processes, Special Periodical Report*; Chemical Society: London, 1975; Vol. 2, p 151.
(13) Johari, G. P.; Goldstein, M. *J. Chem. Phys.* **1970**, *53*, 2372.
(14) Murthy, S. S. N.; Sobhanadri, J.; Gangasharan *J. Chem. Phys.* **1994**, *100*, 4601.
(15) Gangasharan; Murthy, S. S. N. *J. Chem. Phys.* **1993**, *99*, 9865.
(16) Amoureux, J. P.; Castelain, M.; Benadda, M. D.; Bee, M.; Sauvajol, J. L. *J. Phys.* **1983**, *44*, 513.
(17) Suga, H.; Seki, S. *J. Non-Cryst. Solids* **1974**, *16*, 171.
(18) Sorai, M.; Seki, S. *Mol. Cryst. Liq. Cryst.* **1973**, *23*, 299.
(19) Adachi, K.; Suga, H.; Seki, S. *Bull. Chem. Soc. Jpn.* **1972**, *45*, 1960.
(20) Dworkin, A.; Fuchs, A. H.; Ghelfenstein, M.; Szwarc, H. *J. Phys., Lett.* **1982**, *43*, 121.
(21) Huffman, H. M.; Todd, S. S.; Oliver, G. D. *J. Am. Chem. Soc.* **1949**, *71*, 584.
(22) Hill, N. E.; Vaughan, W. E.; Price, A. H.; Davies, M. *Dielectric Properties and Molecular Behaviour*; Van Nostrand Reinhold: London, 1969.
(23) Corfield, G.; Davies, M. *Trans. Faraday Soc.* **1964**, *60*, 10.
(24) Sherwood, J. N., Ed. *The Plastically Crystalline State*; Wiley/Interscience: New York, 1979.
(25) Krishnaji; Mansingh, A. *J. Chem. Phys.* **1965**, *42*, 2503.
(26) Mansingh, A.; McLay, D. B. *Can. J. Phys.* **1967**, *45*, 3815.
(27) Stockhausen, M.; Hornhardt, S. V. *Z. Naturforsch.* **1992**, *47A*, 1135.
(28) Pathmanathan, K.; Johari, G. P. *J. Phys. C: Solid State Phys.* **1985**, *18*, 6535.
(29) Angell, C. A.; Busse, L. E.; Cooper, E. I.; Kadiyala, R. K.; Dworkin, A.; Ghelfenstein, M.; Szwarc, H.; Vassal, A. *J. Chim. Phys. Phys.-Chim. Biol.* **1985**, *82*, 267.
(30) White, A. H.; Biggs, B. S.; Morgan, S. O. *J. Am. Chem. Soc.* **1940**, *62*, 16.
(31) Turney, A. *Proc. IEE, II A* **1953**, *100*, 46.
(32) White, A. H.; Bishop, W. S. *J. Am. Chem. Soc.* **1940**, *62*, 8.
(33) Aihara, A.; Kitazawa, C.; Nohara, A. *Bull. Chem. Soc. Jpn.* **1970**, *43*, 3750.
(34) Hall, P. G.; Horsfall, G. S. *J. Chem. Soc., Faraday Trans. 2* **1974**, *69*, 1071.
(35) Brot, C.; Darmon, I. *J. Chem. Phys.* **1970**, *53*, 2271.
(36) Ries, H.; Böhmer, R.; Fehst, I.; Loidl, A. *Z. Phys. B* **1996**, *99*, 401.

(37) Tan, Z.; Nakazawa, Y.; Saito, K.; Sorai, M. *Bull. Chem. Soc. Jpn.* **2001**, *74*, 1221.
(38) Ramos, J. J. M.; Correia, N. T. *Mol. Cryst. Liq. Cryst.* **2003**, *404*, 75.
(39) Correia, N. T.; Ramos, J. J. M.; Diogo, H. P. *J. Phys. Chem. Solids* **2002**, *63*, 1717.
(40) Shahin, Md.; Murthy, S. S. N. *J. Chem. Phys.* **2003**, *118*, 7495.
(41) Shahin, Md.; Murthy, S. S. N. *J. Chem. Phys.* **2005**, *122*, 14507.
(42) Havriliak, S.; Negami, S. *J. Polym. Sci. C* **1966**, *14*, 99.
(43) Murthy, S. S. N. *J. Phys. Chem. B.* **1997**, *101*, 6043. The exact identity between f_m and f_0 is, $f_m = f_0[k'/(\cos(\alpha\pi/2) - \sin(\alpha\pi/2)\cdot k')]^{1/(1-\alpha)}$, where $k' = \tan([(1 - \alpha)\pi]/[2(1 + \beta)])$.
(44) Murthy, S. S. N. *J. Phys. Chem.* **1989**, *93*, 3347.
(45) Murthy, S. S. N. *J. Mol. Liq.* **1990**, *47*, 1.
(46) Murthy, S. S. N.; Paikaray, A.; Arya, N. *J. Chem. Phys.* **1995**, *102*, 8213.
(47) Matsuoka, M.; Ozawa, R. *J. Cryst. Growth* **1989**, *96*, 596.
(48) Wiedemann, H. G.; Bayer, G. *J. Therm. Anal.* **1985**, *30*, 1273.
(49) Murthy, S. S. N.; Kumar, D. *J. Chem. Soc., Faraday Trans.* **1993**, *89*, 2423.
(50) Murrell, J. N.; Jenkins, A. D. *Properties of Liquids and Solutions*, 2nd ed.; John Wiley: Chichester, UK, 1994.
(51) Murthy, S. S. N.; Tyagi, M. *J. Chem. Phys.* **2002**, *117*, 3837.
(52) Johari, G. P. *Philos. Mag. B* **1980**, *41*, 41.
(53) Tyagi, M.; Murthy, S. S. N. *J. Phys. Chem. A* **2002**, *106*, 5072.
(54) Murthy, S. S. N. *Phase Transitions* **2002**, *75*, 487.
(55) Tajima, Y.; Matsuo, T.; Suga, H. *J. Phys. Chem. Solids* **1982**, *45*, 1165.
(56) Tanaka, I.; Iwasaki, F.; Aihara, A. *Acta Crystallogr. B* **1974**, *30*, 1546.
(57) Rössell, H. J.; Scott, H. G. *Mol. Cryst. Liq. Cryst.* **1972**, *17*, 275.
(58) The specific indexing program chosen for this purpose is TREOR [Werner, P. E.; Ericsson, L.; Westdahl, M. TREOR, a Semi-Exhaustive Trial-and-Error Powder Indexing Program for All Symmetries. *J. Appl. Crystallogr.* **1985**, *18*, 367]. The reader may also refer to Shirley, R. *The Crysfire 2002 System for Automatic Powder Indexing: User's Manual*; The Lattice Press: Surrey, England, 2002.
(59) Marsh, P.; Williams, D. E. *Acta Crystallogr. B* **1981**, *37*, 705.
(60) Charbonneau, G. P.; Trotter, J. *J. Chem. Soc. A* **1967**, 2032.
(61) Charbonneau, G. P.; Trotter, J. *J. Chem. Soc. A* **1968**, 1267.
(62) Decressain, R.; Carpentier, L.; Cochin, E.; Descamps, M. *J. Chem. Phys.* **2005**, *122*, 034507.
(63) Willart, J. F.; Descamps, M.; Benzakour, N. *J. Chem. Phys.* **1996**, *104*, 2508.
(64) Yamamuro, O.; Ishikawa, M.; Kishimoto, I.; Pinvidic, J.; Matsuo, T. *J. Phys. Soc. Jpn.* **1999**, *68*, 2969.
(65) Brand, R.; Lunkenheimer, P.; Schneider, U.; Loidl, A. *Phys. Rev. Lett.* **1999**, *82*, 1999.